JOURNAL OF MATERIALS SCIENCE 23 (1988) 4541–4546

IR and Raman studies and effect of γ radiation on crystallization of some lead borate glasses containing Al_2O_3

SHANKAR RAM
Advanced Centre for Materials Science, Indian Institute of Technology, Kanpur-208016, India
KANIK RAM
DMSRDE, Kanpur-208013, India

IR and Raman spectra of glass ceramics based on $PbO–Cr_2O_3–B_2O_3$ glass composition system have been studied. The bands characteristic of BO_3 and BO_4 functional groups are present in all the samples. An incorporation of Al_2O_3 (up to ~5 mol%) in the initial glass composition considerably changes the glass network structure and relative concentrations of BO_3 and BO_4 groups. The composition 50 PbO–20 Cr_2O_3–25 B_2O_3–5 Al_2O_3 (in mol%) reveals a maximum fraction of boron in the BO_4 group. A sample of this composition heat treated at 850° C for 25 h shows a maximum crystallization fraction with $Pb_2O \cdot CrO_4$ as a prominent crystalline phase. The glasses irradiated with γ rays inhibit the crystallization into the $Pb_2O \cdot CrO_4$ phase. They also show relatively smaller thermal conductivity.

1. Introduction

The crystallization behaviour of transition metal alloys and oxide glasses has been investigated from several points of view, such as thermal stability for commercial applications, effects on magnetic properties, and kinetics of transformation from the amorphous to the crystalline phase. Much effort has been devoted to delineating the morphology and crystallography of crystals precipitated in the glasses by heat treatments [1–3]. Recently, we have reported the crystallization properties of $PbO–Cr_2O_3–B_2O_3$ glasses [4]. Pb_2CrO_5 microcrystals readily precipitate out in the system as red needles upon heat treatments between 500 and 1000° C. An addition of small amounts of Al_2O_3 in the system increases nucleation giving rise to a dramatic increase in the crystallization volume fraction [4]. Glass ceramics containing appreciable amounts of the lead chromate particles are especially useful for fibre optics, laser hosts, acousto-optical devices, magneto-optic switches and lead acid battery electrodes [5–7].

In this investigation we report a detailed analysis of the IR and Raman spectra and the thermal conductivity data with an attempt to understand the crystallization process and short range structures of the system. After irradiation with γ-rays the glasses exhibit lower thermal conductivities. The results are discussed in terms of the proposed model for the glass structures.

2. Experimental details

The compositions of the $PbO–Cr_2O_3–B_2O_3–Al_2O_3$ glass investigated are given in Table I. The mixed oxide chemicals (reagent grade) are melted at ~1100° C for 2 h. The molten glass is poured between two stainless steel plates and pressed into thin (~0.2 cm) platelets. The samples are then given heat treatments in order to obtain the ceramized glasses. We have also studied the effect of γ-irradiation on the glass specimens. The irradiation is carried out by a ^{60}Co source at a dose rate ~1.5 Mrad h^{-1} with dose of 0.5 to 300 Mrad.

IR spectra (200–4000 cm^{-1}) are taken of powder samples in KBr pellets on a Perkin Elmer 783 spectrophotometer. The Raman spectra are recorded by a Spex 1403 Ramalog spectrophotometer using 514.5 nm line of an Ar^+ laser for the excitation. The low temperature measurements (between 300 and 77 K) are accomplished by mounting the sample (in a capillary) in a Hornig-type dewar and using liquid nitrogen as a coolant.

The thermal conductivity measurements are carried out at room temperature (~300 K) by the steady state method [8].

3. Results and discussion

3.1. Infrared and Raman spectra

3.1.1. Structural properties of the glasses

The infrared spectra of $PbO–Cr_2O_3–B_2O_3$ glasses shown in Fig. 1 are usually characterized by two broad (also intense) bands at 300–800 cm^{-1} and 1100–1500 cm^{-1}, and two weak bands at 850 and 1020 cm^{-1}. The features are somewhat similar to those for the pure B_2O_3 glass (cf. Fig. 1a) which exhibits three absorption peaks at 656, 1276 and 1492 cm^{-1}. The vitreous B_2O_3 is believed to form $(B_3O_{4.5})_\infty$ boroxol rings bonded irregularly to one another [9]. The band structures and intensities are modified in the glasses containing small amounts of Al_2O_3. The band group at ~1020 cm^{-1} (doublet structure) grows in intensity and shifts to

0022–2461/88 $03.00 + .12

TABLE I Composition of glasses

Glass number	Glass classification	Mol % of constituents			
		B_2O_3	Cr_2O_3	PbO	Al_2O_3
G_0	Base glass (G_0)	30	20	50	0
$G_{0.5}$	G_0 + 0.5 Al_2O_3	29.5	20	50	0.5
G_1	G_0 + 1 Al_2O_3	29.0	20	50	1.0
G_2	G_0 + 2 Al_2O_3	28.0	20	50	2.0
G_3	G_0 + 3 Al_2O_3	27.0	20	50	3.0
G_5	G_0 + 5 Al_2O_3	25.0	20	50	5.0
G_{10}	G_0 + 10 Al_2O_3	25.0	20	45	10.0

higher frequencies with increasing Al_2O_3 content to ~ 5 mol %. The area of the absorption within 300–800 cm^{-1} decreases regularly and relatively sharp bands appear at ~ 590 and 700 cm^{-1} in the glass G_5 (5 mol % Al_2O_3). The glass compositions with higher (> 5 mol %) Al_2O_3 content further reveal very broad features at ~ 550 cm^{-1}, 1060 cm^{-1} and 1430 cm^{-1} (glass composition G_{10}). Also, the 1060 cm^{-1} band comprises a considerably enhanced intensity. The heat-treated glasses (spectra e–g in Fig. 1) exhibit several new bands with sharp structures. This clearly indicates crystallization of the system after heat treatments.

The broad features in the 1250 and 650 cm^{-1} regions are definitely due to the BO_3 group forming the boroxol ring (Fig. 2). The relatively sharper and weaker bands observed in case of glass G_5 (also heat-treated samples) reveal a change of boron coordination from three (BO_3) to four (BO_4), the latter group would have an inherently higher local site symmetry [10]. The free BO_4 ion (T_d symmetry) has four modes of vibration [10]; symmetric stretching $\nu_1(A_1) \sim 750$ cm^{-1}, asymmetric stretching $\nu_3(F_2) \sim 1030$ cm^{-1} and deformation modes $\nu_2(E) \sim 380$ cm^{-1} and $\nu_4(F_2) \sim 520$ cm^{-1}. E and F_2 refer to double and triple degenerate vibrations, respectively. All four modes are allowed in the Raman spectrum while only the ν_3 and ν_4 are allowed in the IR. In the boroxol ring, a BO_4 group can be incorporated in several ways [9], and the growth of the frequency observed at ~ 1020 cm^{-1} in the glasses containing Al_2O_3 up to ~ 5 mol % represents the $\nu_3(BO_4)$ vibration. This is believed to arise due to the generation of BO_4 groups in the system with diborate or triborate units (Fig. 3).

An IR frequency at 720 cm^{-1} has been reported for the $\nu_2(BO_3)$ vibration (deformation mode) in lanthanide [11] and transition metal [12] borates. In the present investigation, we also assign the sharp band at ~ 720 cm^{-1} in the glass G_5 to this vibration.

A summary of the prominent IR bands due to BO_3 and BO_4 groups in the borate glasses as reported by various authors is given in Table II. The broad absorption between 1100–1500 cm^{-1} region accounts for the $\nu_3(BO_3)$ modes. The shift of this absorption region to still higher frequencies and an appearance of the prominent absorption at ~ 1060 cm^{-1} ($\nu_1(BO_3)$ mode) in glass G_{10} reveals an increase of BO_3 groups in the system probably due to the formation of a tetraborate unit (Fig. 4) (structural units with fewer BO_4 groups than in the triborate). The long chain growth on tetraborate units would, however, be restricted by the high amount of PbO present in the system.

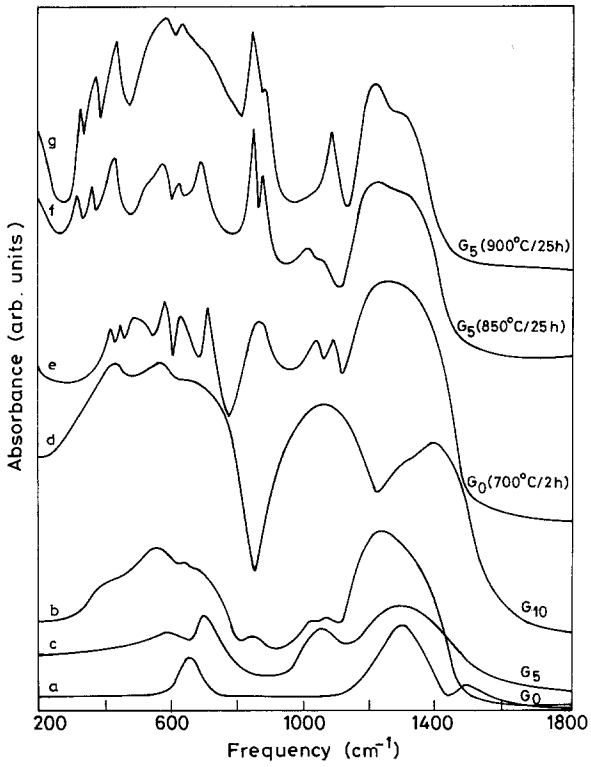

Figure 1 Infrared spectra of PbO–Cr_2O_3–B_2O_3 glass systems; (a) Pure B_2O_3 glass, (b) Glass G_0, (c) G_5 and (d) G_{10}. (e)–(g) Heat treated glasses.

The spectral features of the glass G_{10} can be compared with those for the orthoborates (orthorhombic structure, with the space group D_{2h}^{12}, $z = 2$ and the anions on C_s sites [11]). Here, the ν_1 mode could also exhibit a large IR intensity due to a distortion of BO_3 group symmetry. This distortion is more probable in the glasses of high modifier (PbO and Cr_2O_3) levels [17].

Raman spectroscopy has been more informative about the microstructure of the vitreous borate [15] and alkali borate glasses [9, 15, 16] and this produces a convenient starting point for interpreting the spectra of lead borate glasses in the present investigation. The B_2O_3 glass which is a three-dimensional network of BO_3 triangles polymerized by corner sharing oxygen atoms reveals two groups of bands which primarily involve oxygen motion. The prominent one observed at ~ 806 cm^{-1} corresponds to the breathing mode [9] of the boroxol ring; the simplest model for the glass network. The other frequency at ~ 1250 cm^{-1} (weak intensity) involves the asymmetric motion of an oxygen atom along the B . . . B direction. This band is very sensitive to the B–O–B bond angle and the B–O

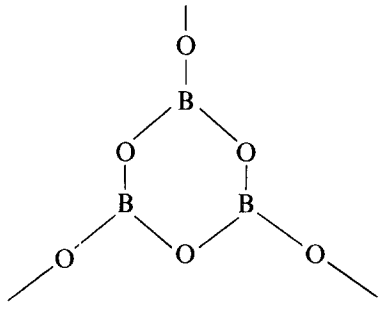

Figure 2 Schematic representation of boroxol ring $(B_3O_{4.5})^{3-}$ in the system.

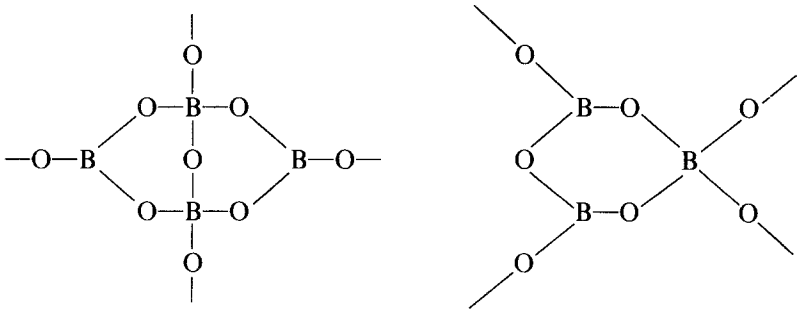

Figure 3 Structures of (a) diborate and (b) triborate units.

bond length. In lead borate glasses, wherein BO_4 groups are also present, the interaction would be between neighbouring BO_4 and BO_3 groups and coupling can be expected to be considerably smaller than between the two BO_3 groups in a pure borate glass. So, as a model, we can treat the framework vibrations as primarily centred on BO_3 and BO_4 polyhedra modified by a perturbation due to their coupling. Fig. 5 shows the Raman spectra of the various $PbO–Cr_2O_3–B_2O_3–Al_2O_3$ glass samples. The content of Al_2O_3 in the system produces a dramatic change in the band positions and relative intensities. The prominent band at $\sim 810\,cm^{-1}$ (corresponding to $\sim 806\,cm^{-1}$ band in pure B_2O_3 glass) progressively disappears and a new band develops at $\sim 780\,cm^{-1}$. Here, a close similarity appears with the Raman spectra of alkali borate glasses and the band at $780\,cm^{-1}$ can accordingly be ascribed to the symmetric breathing vibration in a diborate unit [9, 15, 16].

On further increase of Al_2O_3 content, a broad Raman peak at $765\,cm^{-1}$ appears in the glass G_{10}. For $Li_2O–2B_2O_3$ glasses, Irion *et al.* [15] have correlated this band to the growth of BO_4 groups in the formation of ditriborate and also possibly the diborate units. We comment on this assumption that crystalline $Li_2O–2B_2O_3$ and $ZnO–2B_2O_3$ both contain diborate units only, but their Raman spectra are quite different [18]. Also, the latter does not show strong band features around $765\,cm^{-1}$. Our IR data (discussed above) clearly show a decrease of the BO_4 groups in the $PbO–Cr_2O_3–B_2O_3$ glasses for Al_2O_3 content greater than 5 mol %, and the configurational unit is most probably a tetraborate. The fact is that the Raman band in question represents a symmetric breathing vibration in the tetraborate unit; the vibration being localized mainly on the polyhedron of the first two rings attached by a four coordinated boron (cf. Fig. 4). A similarity with the naphthalene molecule appears (two benzene rings are attached adjacently). The breathing mode in naphthalene [19] exhibits a Raman frequency at $770\,cm^{-1}$ ($1010\,cm^{-1}$ in benzene). The increased mass of the polyhedron could account for a decrease in the band frequency as compared with that for the triborate unit. A bandwidth increase is likely due to a vibrational coupling whose chances are more favourable in the reduced effective symmetry of the vibrational unit in the present case. Also the new bands at ~ 520, 950 and $1100\,cm^{-1}$ occur in the

TABLE II Assignments of prominent IR bands in borate glasses as suggested by various authors

Frequency (cm^{-1}) (1)	Mode of vibration (2)	Reference (3)	Structural unit (4)
BO_3 group modes			
1400	B–O–B stretching in BO_3 with no non-bridging oxygen.	[9]	B_3O_6
1250–1500	B–O stretching in boroxol ring with three non-bridging oxygens.	[9, 15]	–
1250	B–O stretching in BO_3 involving the oxygen connecting the groups; BO_3 triangle (isolated).	[13, 14] [15]	–
650–700	BO_3 bending.	[13, 14]	$(B_3O_6)^{3-}$, $(B_4O_9)^{4-}$
BO_4 group modes			
1350–1380	B–O stretching in BO_4 with one or two non-bridging oxygens.	15	$(B_3O_7)^{4-}$, $(B_3O_8)^{5-}$
1000	B–O stretching in BO_4 with one non-bridging oxygen.	16	$(B_4O_9)^{4-}$
	B–O stretching in an isolated tetrahedron lies at still lower frequencies.		$(BO_4)^{4-}$
900	B–O stretching in BO_4 involving the oxygens connecting the groups.	[13]	$(B_4O_9)^{4-}$
780*	Symmetric breathing vibration of a six membered borate ring with one BO_4 group.	[9, 15]	$(B_3O_7)^{4-}$
650–300	B–O–B bending and borate ring deformation in various borate groups.	[9]	–

*Bands prominent in Raman spectrum.

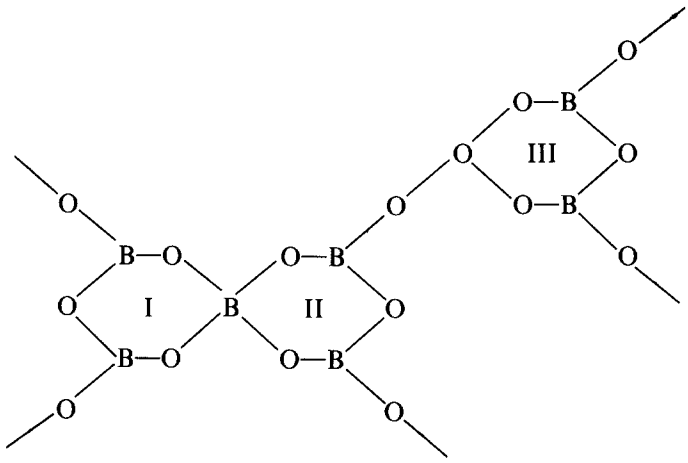

Figure 4 Tetraborate unit.

glass G_{10}. The origin of these bands is not very clear. However, they can most probably be attributed to isolated triangular orthoborate units, which are common in borate glasses [17].

3.1.2. Crystallization and effects of Al_2O_3 as a nucleation catalyst

The $PbO–Cr_2O_3–B_2O_3$ glass systems are amorphous for B_2O_3 content to ~25 mol %. Their X-ray powder diffraction patterns do not reveal any peak [4]. The specimens given heat treatment between 500 and 1100° C are readily crystallized with (1) $PbCrO_4$, (2) Pb_2CrO_5, (3) Cr_2O_3 and (4) PbB_2O_5 respectively as the various crystalline phases [4]. Addition of Al_2O_3 increases nucleation and growth of Pb_2CrO_5 microcrystals at the expense of the two other chromium containing phases when the system is heat treated. The X-ray peaks characteristic of only the Pb_2CrO_5 phase appear in glass G_5 (5 mol % Al_2O_3) after heat treatment at 850° C for 25 h. A maximum crystallized volume fraction of ~80% could be obtained for this sample. Such a catalytic effect of Al_2O_3 is also reported for $ZnO–B_2O_3–SiO_2Al_2O_3$ glasses wherein it promotes the crystallization of the $2Al_2O–B_2O_3$ phase [20]. The IR spectra (Fig. 1) for the heat treated glasses (G_0' and G_5') clearly reveal the reasons for the difference. The IR band at ~860 cm^{-1} is more pronounced in sample G_5'. This band is obviously attributed to the CrO_4^{2-} ion [21]. The bands characteristic of $Pb_2O \cdot CrO_4$ (Pb_2CrO_5) can be identified from the spectra taken of the samples bleached in weak hydrochloric acid. The bleached samples do not contain the bands of borate groups and the spectrum appears to be very simple. Table III summarizes the assignments of all four group modes of CrO_4^{2-}. The degeneracies of ν_2(E) and ν_3, $\nu_4(F_2)$ modes are completely removed indicating thereby that the CrO_4^{2-} in $Pb_2O \cdot CrO_4$ particles have an essentially lower site symmetry than of a T_d. The most probable site symmetry which could explain the observed band splitting patterns is a C_s or C_2. This is consistent with the crystallographic data, i.e., that Pb_2CrO_5 crystallizes in a monoclinic structure with space group $C_{2h}^3 - c^2/m$, $z = 4$ [23].

A most striking feature of the present investigation is that a drastically enhanced crystallization occurs for the system containing 5 mol % Al_2O_3. It appears that the Al_2O_3 changes the relative concentrations of boron present in BO_3 and BO_4 groups by modifying the glass network structure. To speculate on the problem we have plotted in Fig. 6 the intensity ratio $I_4/(I_3 + I_4)$

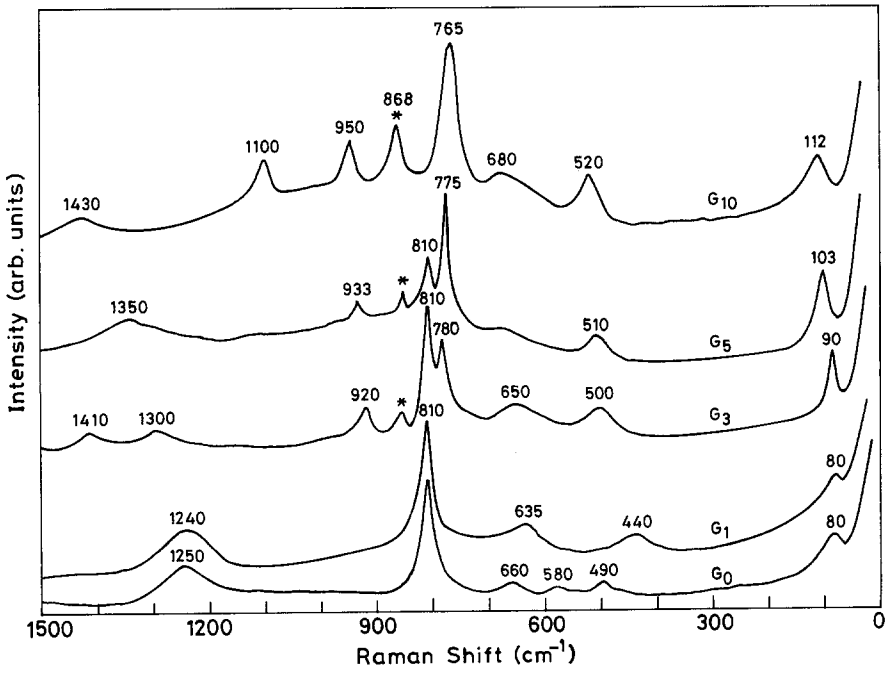

Figure 5 Raman spectra of the $PbO–Cr_2O_3–B_2O_3$ glasses. * Denotes bands due to CrO_4^{2-} ion.

TABLE III IR and Raman bands (cm^{-1}) observed in $Pb_2O \cdot CrO_4$ microcrystals precipitated in the glass G_5 after heat treatment at 850° C for 25 h*.

IR (solid)	Raman (solid)	CrO_4^{2-} bands in H_2O solution†	Assignments‡
325(vw)	330(w)	348	$\nu_2(E)$
375(ms)	373(ms)	368	$\nu_4(F_2)$
–	380(w)		
865(vs)	860(vs)	847	$\nu_1(A_1)$
890(s)	890(w)§		
–	905(ms)	884	$\nu_3(F_2)$
935(sh)§	933(vs)		

*Samples are bleached with weak hydrochloric acid.
†Raman bands observed in aqueous solution of K_2CrO_4 [22].
‡See [11, 21, 22].
§Bands are too weak and could be observed only at low (liquid nitrogen) temperatures.
Relative intensities are given in parentheses; w, weak; vw, very weak; s, strong; ms, medium strong; vs, very strong; sh, shoulder.

(where I_3 and I_4 are the intensities in the Raman bands at 810 and 780 cm^{-1} representing the BO_3 and BO_4 groups respectively) as a function of Cr_2O_3 content and for different amounts of Al_2O_3 in the system. The plot shows a maximum intensity ratio ~ 0.7 at 20 mol % Cr_2O_3 and 5 mol % Al_2O_3 contents. This gives a rough measure of the fraction (N_4) of four coordinated boron atoms (BO_4 group). In glass G_5 (also see Section 3.1.1.), all the tetrahedral boron (BO_4) so formed are thus virtually incorporated as part of the triborate and/or ditriborate units which involve one or two tetrahedral boron. Here, the value (0.7) of N_4 is much larger than expected on the basis of the model structure. The discrepancy could arise from the fact that the Raman intensity neglects the differences in the Raman cross sections of the various species/modes, and a calculation of N_4 should also involve concentration of the boron systems that do not scatter in the 780–810 cm^{-1} region. Whatever the actual N_4 value is it obviously attains a maximum value in the sample G_5, and the glass network structure developed within this composition is suited for the precipitation of the $Pb_2O \cdot CrO_4$ phase. The triborate ditriborate structural units with BO_4 groups

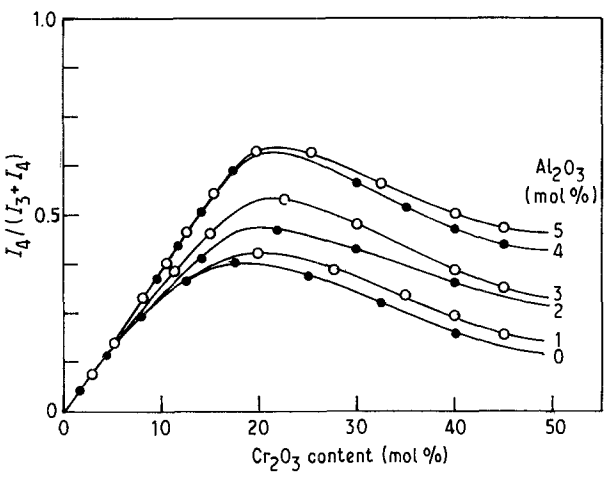

Figure 6 Variation of the intensity fraction $[I_4/(I_3 + I_4)]$ of BO_4 groups in the glass system 70 (PbO–Cr_2O_3)–(30 – X) B_2O_3–X Al_2O_3 as a function of Cr_2O_3 content and with different amounts of Al_2O_3.

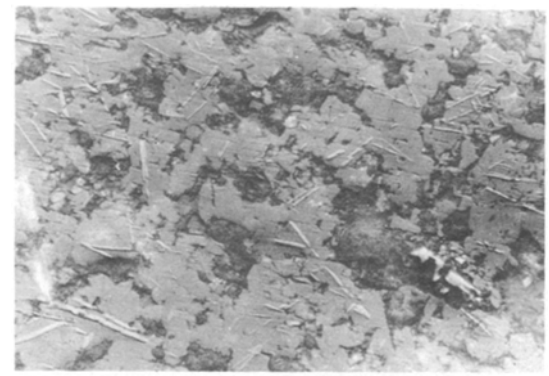

Figure 7 A typical optical micrograph showing the needle-like $Pb_2O \cdot CrO_4$ microcrystals precipitated in glass G_5 after heat treatment at 850° C/25 h. The sample surface is bleached with weak hydrochloric acid. Magnification is 400 times.

probably are symmetrically favourable for the CrO_4^{2-} (tetrahedral) group and thus activate the nucleation and growth of the $Pb_2O \cdot CrO_4$ particles in the system with low activation energy. The Al_2O_3 present in high content (> 5 mol %), on the other hand, behaves as a glass network former and the relative fraction of BO_4 groups decreases (as has been discussed earlier). Small crystallization yields [4] of $Pb_2O \cdot CrO_4$ obtained in these samples support this interpretation.

3.2. Microstructure, thermal conductivity and γ-irradiation effect

The glasses irradiated with gamma rays inhibit the crystallization of the any chromium containing phase. Fig. 7 shows a typical microstructure taken on a Zeiss optical microscope [3] of sample G_5 after heat treatment at 850° C for 25 h. The needle-like precipitated particles are $Pb_2O \cdot CrO_4$ crystals [23]. No such particles could be noted for the specimens irradiated with gamma rays and then given heat treatment. The IR and Raman spectra of these samples also do not exhibit the intense bands from the CrO_4^{2-} group in the crystalline $Pb_2O \cdot CrO_4$ phase. The irradiated glasses probably have some defect centres that prevent the crystallization with $Pb_2O \cdot CrO_4$ crystals. However, we have not been able to identify these centres in this investigation. The spectral measurements carried out

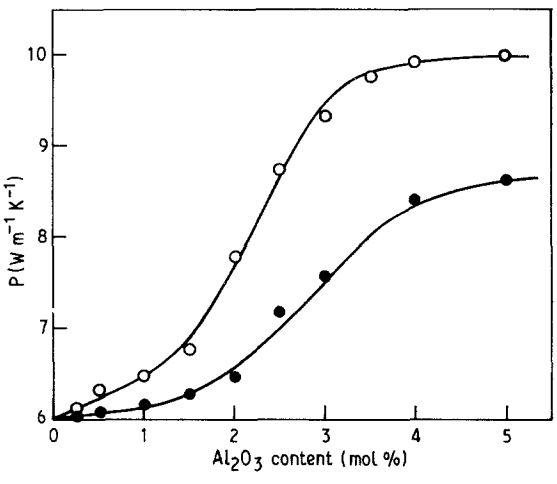

Figure 8 Thermal conductivity of 50 PbO–20 Cr_2O_3–(30 – X) B_2O_3–X Al_2O_3 glasses; (○) before and (●) after gamma irradiation.

on the different irradiated glasses show almost similar band structures irrespective of the Al_2O_3 contents. The relative concentrations of the BO_3 and BO_4 group bands are essentially the same as in glass G_0.

Thermal conductivities (ϱ) of the $PbO-Cr_2O_3-B_2O_3-Al_2O_3$ glass composition systems are measured before and after irradiation with gamma rays. The ϱ value increases with increasing Al_2O_3 content of the glass. It is also observed that the glasses with low PbO content have higher conductivities. The γ irradiation is observed to decrease the thermal conductivity for all the glass compositions studied. Fig. 8 shows the variation of ϱ as a function of the Al_2O_3 content in the system. A dramatic change in conductivity occurs for Al_2O_3 between 1.5 and 3.5 mol %. It steadily increases thereafter to ~ 5 mol % of Al_2O_3. The irradiated glasses follow similar patterns with clearly reduced ϱ values.

In conclusion, the thermal conductivity is very sensitive to the nucleation/growth kinetics and the gamma rays irradiation after effects of the borate glasses. The propagation of heat (similar to light) in solids is governed by the crystal symmetry and basic nature of the material. The amorphous materials exhibit much lower thermal conductivities than the crystals due to a lack of long range periodicity in the structure [24]. In the borate glasses, the variation of the boron structural units with Al_2O_3 content seems to be responsible for a variation of the thermal conductivity. Our experimental results can be explained by the fact (discussed in the preceeding section) that as the Al_2O_3 content increases (up to 5 mol%) the glass structure attains a greater uniformity of the glass network with BO_3 and BO_4 groups on which structural stability and an increased heat-transfer character (ϱ) of the system depend. The gamma irradiated glasses exhibit disordered structure [17, 25]. This causes a short mean free path [25] for the lattice phonon vibrations (heat-transfer carriers) and thereby decreases the conductivity of the glass.

4. Conclusion

Addition of Al_2O_3 (up to 5 mol %) in the $PbO-Cr_2O_3-B_2O_3$ glass system modifies the network structural units causing a change of boron coordination from three (BO_3) to four (BO_4). The fraction of boron atoms in the BO_4 groups is a maximuim in the system containing 5 mol % Al_2O_3. This favours the growth of $Pb_2O \cdot CrO_4$ microcrystals in the system after heat treatment. Irradiation with gamma rays causes a decrease in the short-range order [17, 25] in the glass systems and hence they exhibit lower thermal conductivities and inhibit the crystallization upon heat treatment.

References

1. P. W. McMILLAN, "Glass Ceramics" (Academic, New York, 1979)
2. T. WATANABE and M. SCOTT, *J. Mater. Sci.* **15** (1980) 1131.
3. S. RAM, D. CHAKRAVORTY and D. BAHADUR, *J. Magn. Magn. Mater.* **22** (1986) 221.
4. S. RAM and K. A. NARAYAN, *Ind. Eng. Chem. (Product Research Development)* **26** (1987) 1051.
5. G. BLASSE, *J. Inorg. Nucl. Chem.* **29** (1967) 266.
6. F. KELLENDONK and G. BLASSE, *J. Chem. Phys.* **75** (1981) 561.
7. B. F. MENTZEN, A. LATRACH, J. BOUIX and A. W. HEWAT, *Res. Bull.* **19** (1984) 549.
8. N. A. GHONEIM, *Sprechsaal* **113** (1980) 610.
9. T. W. BRIL, *Philips. Res. Suppl.* **2** (1976) 34.
10. S. D. ROSS, "Inorganic Infrared and Raman Spectra", (McGraw-Hill, Maidenhead, 1972).
11. C. E. WEIR and E. R. LIPPINCOTT, *J. Res. Nat. Bur. Stds.* **65A** (1961) 173.
12. J. P. LAPERCHES and P. TARTE, *Spectrochim. Acta* **22** (1966) 1201.
13. N. TOHGE and J. D. MACKENZIE, *J. Noncryst. Solids* **68** (1984) 411.
14. A. S. TENNY and J. WANG, *J. Chem. Phys.* **56** (1972) 5516.
15. M. IRION, M. CAUZI, A. LEVASSEUR, J. M. REAU and J. C. BRETHOUS, *J. Solid State Chem.* **31** (1980) 285.
16. Y. ITO, K. MIYAUCHI and T. OI, *J. Noncryst. Solids* **57** (1983) 389.
17. A. J. LEADBETTER and A. C. WRIGHT, *Phys. Chem. Glasses* **18** (1977) 18.
18. W. L. KONIJNEDIJK, *Philips Res. Rep. Suppl. No. 1* (1975).
19. K. H. MICHAELIAN and S. M. ZIEGLER, *Appl. Spectrosc.* **27** (1973) 13.
20. W. TIE, H. OULI, X. ZENGZOU, G. FANGTIAN and Z. AO, *J. Noncryst. Solids* **80** (1986) 215.
21. W. P. DOYLE and P. EDDY, *Spectrochim. Acta* **23A** (1967) 1903.
22. H. STAFSUDD, D. BASSI and O. SALA, *ibid.* **12** (1958) 403.
23. J. C. RUCKMAN, R. T. W. MORRISON and R. H. BUCK, *J. Chem. Soc. (Dalton Trans.)* **1** (1972) 426.
24. D. G. HOLLOWAY, "Physical Properties of Glasses" (The Wykeham, London, 1973) p. 41.
25. T. L. SMITH, P. J. ANTHONY and A. C. ANDERSON, *Phys. Rev. B.* **17** (1978) 4997.

Received 15 April
and accepted 22 October 1987